PAPER • **OPEN ACCESS**

Comparison of different correlative AFM-SEM workflows on calcite moonmilk

To cite this article: S Dinarelli *et al* 2022 *IOP Conf. Ser.: Mater. Sci. Eng.* **1265** 012011

Comparison of different correlative AFM-SEM workflows on calcite moonmilk

S Dinarelli[1], F Mura[1,2], C Mancini[1], G La Penna[1], T Rinaldi[2,3] and M Rossi[1,2]

[1] Department of Basic and Applied Science, Sapienza University of Rome, Rome, Italy
[2] CNIS - Center on Nanotechnology Applied to the Engineering of Sapienza, Sapienza University of Rome, Rome, Italy
[3] Departiment of Biology and Biotechnology, Sapienza University of Rome, Rome, Italy

E-mail: francesco.mura@uniroma1.it

Abstract. In recent years, high resolution microscopy techniques are evolving toward a fast combination of different microscopies and spectroscopies, generally labelled under the title of correlative microscopy, each capable to provide unique information and a more comprehensive characterization of the sample under analysis. Among them stands out the Correlative Probe to Electron Microscopy (CPEM), where Scanning Electron Microscopy and Scanning Probe Microscopy are combined. This kind of technique is relatively new, and its range of capabilities is still not fully explored. In this paper, a demonstration of different CPEM workflows to characterize the moonmilk, a particular type of nanostructured calcium carbonate, extracted from ancient tombs of the Etruscan Necropolis of Tarquinia, is provided. Besides, the advantages of an innovative AFM-in-SEM setup, even respect to the standard standalone AFM measurement, are presented, showing how the analysis of the moonmilk nano-fibers, a rather challenging sample to be analysed with probe microscopies, is simplified and with less risk of artefacts or contamination of the AFM probe.

1. Introduction

During the last decade, the so-called correlative microscopy has gained increasing relevance in both research and industry, providing not only a strong impulse for the creation of new specific instrumentation, but also towards the development of rapid and effective analysis protocols for its application [1]. The key component of this experimental approach is the precise and fast localization of the very same features among the different microscopic and spectroscopic techniques in use. This is not always straightforward and, essentially, it can be performed following two different approaches: (a) to implement "in-situ" several techniques and perform the measurement at the same time or sequentially without moving the sample or (b) implement a strategy to localize the same region of the sample while physically moving it among the different instrumentations, for example by means of localizing grids or markers. The first and most known example of correlative microscopy is the CLEM – Correlative Light to Electron Microscopy – where the high-resolution imaging of the electron microscope is correlated with a fluorescence optical analysis, thus granting the possibility to highlight information regarding the internal functions of cells and tissues [2]. However, not only light and electron microscopies can be combined, but by adopting specific protocols, a great number of combinations with different characterizing techniques, such as Raman or Atomic Force Microscope (AFM) can be done [3,4]. All the available configurations make the correlative microscopy a very powerful tool, capable to improve the knowledge of complex phenomena that can't be achieved by the standalone microscopies, while, at

the same time, it avoids dispersion of data due to different sample preparations and treatments [1]. Moreover, this approach is not limited only to a normal bidimensional analysis, but it can be arranged also to perform a complete 3D reconstruction of a sample, by combining, for example, X-Ray tomography with Focused Ion Beam and Electron Tomography [5]. In this paper we take advantage of the capabilities of a recently developed correlative microscopy that is called CPEM – Correlative Probe to Electron Microscopy –, that consists in the combination of Scanning Electron Microscopy (SEM) with a Scanning Probe Technique [6,7]. In our experimental configuration, we have an AFM operating in tapping mode placed inside the chamber room of the electron microscope. In this way, SEM imaging is used to quickly navigate the sample and localize the Region of Interest (ROI) in which the AFM measurement will be performed. Besides, during the AFM scan, the electron beam is maintained on and focused a few nanometers away from the tip, generating a very slow SEM image in parallel with AFM measurement. This gap between the tip and the electron beam is necessary to avoid the disturbance of the tip itself (shadowing effect) [8]. Then, from the overlapping of these two images, it is possible to obtain a final CPEM image that condensate on the very same area, all the information typical of the SEM imaging with the real height values measured with the AFM. However, it is worth mentioning that the AFM can be used not only to measure the height, but also others specific physical properties such as local elasticity or local conductivity [9]. In this paper, we used Raman spectroscopy, AFM and SEM to characterize two different samples of moonmilk, a particular type of nanostructured calcium carbonate, sampled from ancient tombs of the Etruscan Necropolis of Tarquinia [10,11]. Moreover, the capabilities of CPEM will be discussed by comparing the results obtained using two different and physically separate SEM and AFM and an innovative AFM-in-SEM system, the Litescope from Nenovision [12]. The rationale of this work is to demonstrate the usefulness of the CPEM technique onto a very challenging samples from the AFM point of view, since moonmilk consists in relatively variable sized objects, deposited onto a rough surface and located at different height planes. This kind of samples can rapidly deteriorate the AFM tip, compromising the whole measurements. In this panorama, it is crucial to avoid performing "blind" AFM analysis, i.e., looking at random region of the sample trying to find the object of interest, but instead, the correlative approach could be an enormous advantage, providing a preliminary zoom in the region of interest with the SEM and directly checking in live mode the position of the AFM tip and start the AFM measurements at the precise desired location.

2. Materials and Methods

2.1. Environmental parameters for the sample collection and SEM\AFM preparation

Moonmilk deposits, about 0,5 gr., were collected from two ancient Etruscan tombs: Tomba degli Scudi and Tomba Maggi located in the Monterozzi Necropolis [13], using sterile scalpels and kept in 10 ml sterile tubes. The relative humidity in the tombs typically varied in the range 95-98% and the temperature between 16-18°C. A little portion of powder containing the sample has been deposited on an aluminium stub, previously cleaned with acetone, partly covered by bi-adhesive tape. The deposition has been performed in such a way that a part of the sample stitch to the tape and a part remains directly on the metal. The obtained stubs have been used throughout all the experiments performed in this paper. Since the two tombs were carved in two different rocks, the samples will be defined according to the rock's substrate name, i.e., Macco (fossiliferous calcarenite) and Sabbione (hybrid sandstone) that belongs to the Tomba Maggi and Tomba degli Scudi, respectively [11,14].

2.2. Instrumentation and setups

2.2.1. Scanning Electron Microscope and Focus Ion Beam

The orientation marker for the ex-situ CPEM workflow has been produced with a Cobra Focused Ion Beam (from Physics D'Orsay), mounted on an Auriga 405 FE-SEM (from Zeiss). The operating condition of the electron microscope for this analysis are 3 kV for the acquisition voltage, 5.5 mm for the working

distance (i.e. the distance between the electron gun and the sample), while high vacuum has been kept at a pressure of 10^{-5}-10^{-6} mbar.

2.2.2. Stand-alone AFM

The AFM stand-alone measurements were performed with an AFM ICON (from Bruker) in two modalities: (a) contact mode while equipped with triangular-shaped silicon nitride cantilever (model DNP), with nominal elastic constant of 0.06 N/m and (b) tapping mode while equipped with rectangular-shaped silicon nitride cantilever (model RTESP) with nominal resonant frequency of 300 kHz and elastic constant of 40 N/m. Both cantilevers ended with a silicon nitride tip with nominal radius of 10 nm. The maximum vertical force used has been set lower than 1 nN to avoid damages to the tip or the sample.

2.2.3. AFM-in-SEM

To acquire in situ CPEM images, a combined system made of SEM VEGA (from TESCAN) and an AFM LiteScope (from Nenovision) has been used. The SEM is equipped with a tungsten's filament while the Litescope module is allocated directly on the sample holder inside the SEM chamber by means of 4 screws and a proprietary adaptor, the complete setup can be seen in [12]. AFM measurements have been performed in tapping mode with a self-sensing and self-actuating tuning-forkbased tip (model Akiyama) with nominal resonant frequency of 45 kHz and nominal elastic constant of 5 N/m. To obtain the SEM micrograph for the final CPEM image, the electron beam is taken active and focused on a position few nanometres away from the tip, to avoid the creation of any kind distortion duethe tip itself, the so-called shadowing effect [8]. Throughout all the characterizations the chamber in maintained in high vacuum at a pressure of 10^{-4} mbar, to grant the possibility of obtaining SEM images of good quality. The acquisition voltage was set to 4-6 kV in such a way to not damage the sample itself or create artifacts in the acquired images, while the working distance was set to around 10mm in order to maximize the signal-to-noise ratio.

2.2.4. Micro-Raman

Raman spectra were collected using a confocal inVia™ Raman Spectrometer (from Renishaw), with 250 mm focal length. The specimens were analyzed at room temperature in the 145-1800 cm^{-1} spectral range. The signal is dispersed by a holographic grating of 1800 l/mm and collected by a Peltier-cooled CCD detector. The excitation line at 532.1 nm was produced by a Nd:YAG continuous-wave diode-pumped solid state laser (from Renishaw) and focused on the sample through a short distance working objective N PLAN 50x, with NA = 0.75 (from Leica Microsystems). The laser power impinging on the samples was set to 25 mW with an exposition time of 0.4s and 15-20 accumulations. For each sample five spectra have been collected. The peak positions were automatically calibrated using an internal reference of a Ne-Ar light available in the spectrometer. The software WiRETM 4.4 has been used to normalize the spectra, perform fitting procedures, and obtain peaks position. Normalized intensities of each band are obtained considering the ratio between their height and the intensity of the most intense band in the spectrum.

3. Results and Discussions

The Etruscan Tombs in the Monterozzi Necropolis of Tarquinia, carved in calcarenite and hybrid sandstone rocks, with constant temperature and humidity, show the presence of nanometric-scale crystals of calcium carbonate in the form of calcite, forming a white patina covering the walls; this speleothem is called moonmilk and, despite its formation has a biogenic origin, the physical mechanism promoting the formation of the nanometric fibres is unknown [14-16]. In previous studies, we analysed a collection of samples from 13 tombs of the archaeological area, and we observed that the rock substrate has a strong influence on the final structures of the moonmilk nanorods, showing, for example, that in

the Tomba degli Scudi, excavated in a hybrid sandstone vein, the moonmilk is made of mostly of single and multiples smooth nanorods [11].

3.1. Raman characterization

The Raman spectroscopy has been performed on the moonmilk samples collected from two Etruscan tombs having a different rock substrate, as further confirmation of the analysis reported in a previous paper [14]. This is a further proof that the shape and size of the nanofibers doesn't change its crystalline structure. In fact, the moonmilk is a biogenic form of the calcite, which is characterized by a rhombohedral geometry, precisely a D_{3d}^6 point symmetry [17], and, according to the group theory of vibrational spectra [18], the Raman spectrum of these minerals is expected to have five fundamental phonons, listed in Table 1.

Table 1. Description of the five fundamental phonons of calcite [19].

Phonon symbol	Wavenumber [cm^{-1}]	Description
E_g(T)	154	*External vibration* due to the interaction between CO_3^{2-} and Ca^{2+}: translations of the CO_3^{2-} group in the primitive cell around the axes normal to the C_3 axis.
E_g(L)	281	*External vibration* due to the interaction between CO_3^{2-} and Ca^{2+}: liberations of the CO_3^{2-} group in the primitive cell around the axes normal to the C_3 axis.
E_g	711	*Internal vibrations* of the CO_3^{2-} group.
A_{1g}	1087	
E_g	1438	
E_g+A_{1g}	1742	A combination band.

The obtained spectra, showed in fig. 1, confirm the presence of the calcite, where the four peaks positions expected in the range 155-1086 cm^{-1} are perfectly overlapped with the reference spectrum, also respecting the intensity ratio among the peaks.

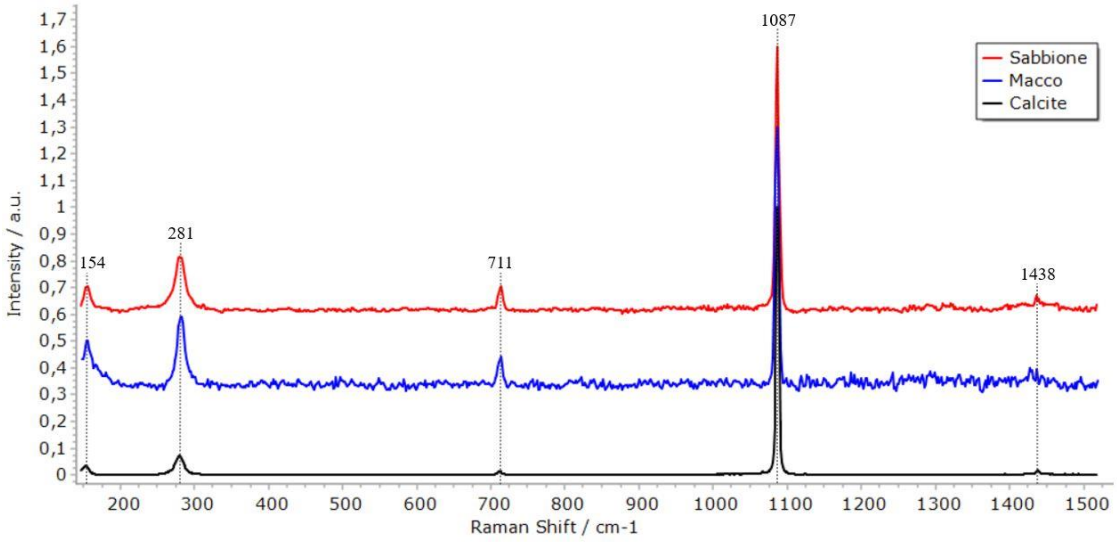

Figure 1. Comparison (in order from top to bottom) between the spectra acquired on Sabbione (red line), Macco (blu line) and reference calcite spectrum from the Renishaw Database (black line) – color online. The spectra are normalized with respect to the peak at 1087 cm^{-1} and stacked with a vertical shift of 0.3 a.u..

3.2. CPEM characterization

The workflow of a typical CPEM measurement operated through a reference marker, as performed in this work, is reported in figure 2.

Figure 2. Subsequent steps to perform a CPEM image on a moonmilk sample using a FIB reference marker. (a) and (b) progressive zoom with the FESEM of the very same region subsequently imaged with the AFM; (c) higher magnification of a single moonmilk nanofiber and (d) corresponding AFM image on the structure of interest acquired with the AFM-in-SEM configuration.

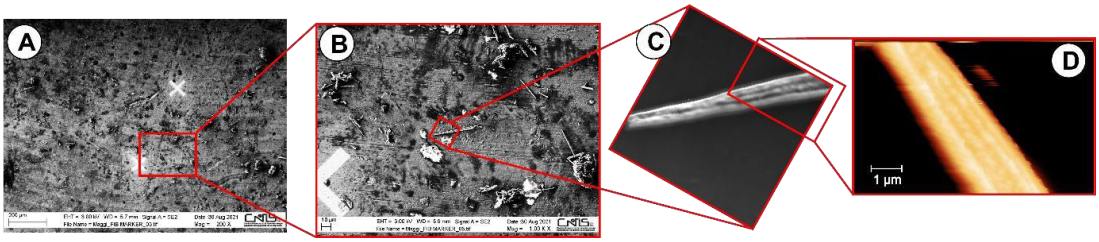

In figure 2(a) and 2(b) are reported two FESEM images of the region of interest taken at different magnifications, where the FIB markers, the two crosses, are clearly visible. The same sample has been transferred to the SEM from TESCAN, to perform the AFM-in-SEM characterizations. In figure 2(c), it's reported a higher magnification of a specific single moonmilk nanofiber, whose image has been rotated respect to its original orientation inside the TESCAN microscope chamber room to give a clear connection with the previous two images of the figure. This area has been later scanned and observed as an AFM image (fig. 2(d)). However, the initial step of the creation of the FIB marker can be avoided, as well as their search through the optical camera of the AFM, by performing an AFM-in-SEM approach. In our case, the Litescope module has been mounted directly inside the chamber room of the SEM, and besides being a timesaving approach to the measurement, it allows to take advantage of the capabilities of the SEM to have a fast scan of the sample and then to have a fast identification of the region of interest. In this way, the AFM image can be acquired with absolute certainty of the positioning of the tip and even with the selection of the right image size. An example of this "in-situ" CPEM approach is shown in fig. 3, where an area of 20 μm^2 containing some moonmilk nanofibers has been analysed.

Figure 3. Composition of a CPEM image: (a) SEM and (b) AFM raw images acquired simultaneously. (c) 2D and (d) 3D representation of the CPEM image.

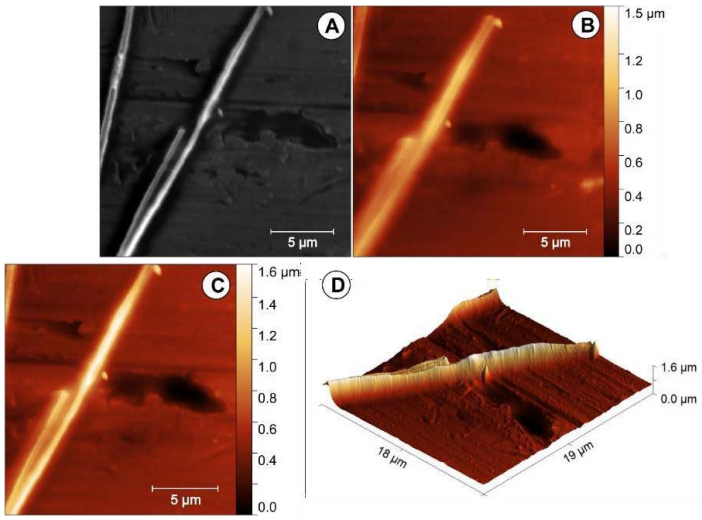

Looking at the fig. 3(a) and 3(b), it's easy to notice that the SEM and AFM images are slightly shifted. This shifting is intrinsic of the technique, since, to make possible the simultaneous acquisition of a SEM image during the AFM scanning, the electron beam is maintained at a fixed distance from the tip, to avoid the shadowing effect. However, this issue is easy to overcome by superimposing the two acquisitions, as shown in fig. 3(c) and 3(d), where the final CPEM image in 2D and 3D view are, respectively, reported. By the comparison of all the pictures exposed in fig. 3, it's easy to notice that CPEM is not only an addition of the qualitative height measurement of the AFM, but an enhanced image able to embed the best from both instruments, resulting into a more complete characterization of the sample.

3.3. Standalone AFM analysis

For comparison, we have analysed the two samples adopting a standard stand-alone AFM approach, where some acquired areas are reported in figure 4.

Figure 4. AFM images acquired with the standalone AFM in air: (a) tapping mode image of Sabbione, (b) contact mode and (c) tapping mode images acquired on the Macco's sample.

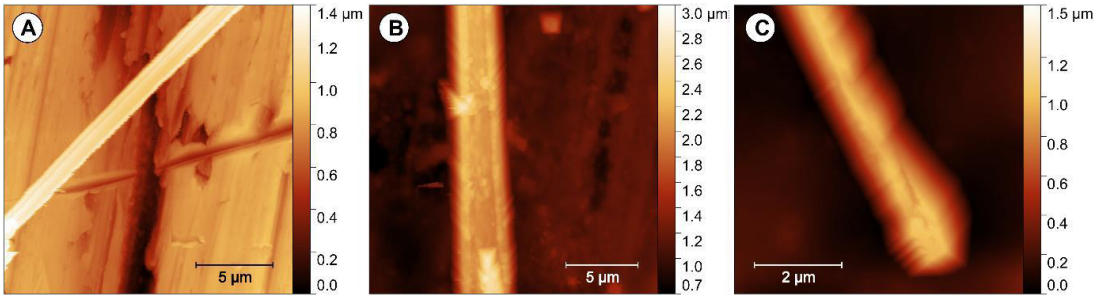

The quality of the images is almost the same as presented in the previous chapter, but with two crucial differences: (a) to obtain an image of a single structure, several areas need to be scanned to locate a structure of interest; (b) once a structure is located, you have no control on the surrounding, and could happen that this nanofiber can be stacked on the top of another, overcoming the z-piezo vertical range. These effects can lead to a fast deterioration of the AFM tip, like collecting dirt from the substrate or even collecting entire pieces of the nanofibers. One example is illustrated in fig. 4(a), where an AFM image of the Sabbione sample in tapping mode is reported. The final image is very neat and sharp, but a small defect can be noted in the bottom left, maybe due to the presence of another superimposed structure. Other examples of tip contamination are shown in figure 4(b) and 6(c), where two different areas have been acquired onto the Macco sample, respectively, in contact and tapping mode. In both cases, the presence of some contaminations on the tip influences the achievable resolution, and it should be noted that the images here reported are the best ones obtained in several days of measurements with the stand-alone AFM, another important evidence of the very challenging nature of these class of samples in Atomic Force Microscopy.

4. Conclusions

In this paper we have reported two different workflows for the CPEM characterization applied to an AFM challenging sample like the moonmilk, illustrating the advantages that arise from a direct measurement through an AFM-in-SEM device. These nanofibers have been extracted from two Etruscan tombs, having a different rock substrates underneath, the Macco for Tomba Maggi and Sabbione for Tomba degli Scudi, which have a great influence on the final shape and size of the moonmilk. The

Raman analysis confirms that they are made of calcite, without showing any kind of variation due to their different morphology. Besides, the capabilities of our AFM-in-SEM system of approaching the CPEM in an easiest and fastest way, as well as ensuring additional information, respect using a traditional AFM or a FIB marker workflow, have been demonstrated. Another important aspect of an in-situ CPEM is the possibility to reduce dramatically the presence of artifacts and contaminations of the tip, that are unavoidable in the standard "blind" AFM analysis. For these reasons, further studies will be devoted to the high-resolution systematic characterization of the two samples, to provide quantitative data on the structural differences, like the roughness, of the different type of moonmilk.

Acknowledgments

This research has been realized with the financial support of the projects CHALLENGES - Real time nano characterization related technologies, granted by European Commission (call H2020-NMBP-TO-IND-2019) and ATOM - Advanced Tomography and Microscopies, granted by Lazio Region (call "Open infrastructures for research").

References

[1] Parlanti P and Cappello V 2022 Microscopes, tools, probes, and protocols: A guide in the route of correlative microscopy for biomedical investigation *Micron* **152** 103182.
[2] Giepmans BNG 2008 Bridging Fluorescence microscopy and electron microscopy *Histochem. Cel. Biol.* **130** pp. 211-217.
[3] Schmidt R, Nachtnebel M, Dienstleder M, Mertschnigg S, Schroettner H, Zankel A, Poteser M, Hutter H, Eppel W and Fitzek H 2021 Correlative SEM-Raman microscopy to reveal nanoplastics in complex environments *Micron* **144** 103034.
[4] Jadavi S, Bianchini P, Cavalleri O, Dante S, Canale C and Diaspro A 2021 Correlative nanoscopy: A multimodal approach to molecular resolution *Microsc. Res. Tec.* **84** pp. 2472-2482.
[5] Ma L, Dowey P, Rutter E, Taylor K and Lee P 2019 A novel upscaling procedure for characterising heterogeneous shale porosity from nanometer-to millimetre-scale in 3D *Energy* **181** pp. 1285-1297.
[6] Holz M, Reuter C, Reum A, Ahmad A, Hofmann M, Ivanov T, Mechold and Rangelow IW 2019 Atomic force microscope integrated into a scanning electron microscope for fabrication and metrology at the nanometer scale *Proc. SPIE Photomask Technology 2019* Vol. 11148 p. 111481F.
[7] Rangelow IW, Kaestner M, Ivanov T, Ahmad A, Lenk S, Lenk C, Guliyev E, Reum A, Hofmann M, Reuter C and Holz M 2018 Atomic force microscope integrated with a scanning electron microscope for correlative nanofabrication and microscopy *Journal of Vacuum Science & Technology B* **36(6)** 06J102.
[8] Fukushima K, Kawai S, Saya D and Kawakatsu H 2002 Measurement of mechanical properties of three-dimensional nanometric objects by an atomic force microscope incorporated in a scanning electron microscope *Rev. Sci. Instrum.* **73(7)** pp. 2647 – 2650.
[9] Novotna V, Horak J, Konecny M, Hegrova V, Novotny O, Novacek Z and Neuman J 2020 AFM-in-SEM as a Tool for Comprehensive Sample Surface Analysis *Microscopy Today* **28(3)** pp. 38-46.
[10] Tomassetti MC, Cirigliano A, Arrighi C, Negri R, Mura F, Maneschi ML, Gentili MD, Stirpe M, Mazzoni C and Rinaldi T. 2017 A role for microbial selection in frescoes' deterioration in Tomba degli Scudi in Tarquinia, Italy *Scientific Reports* **7** 6027.
[11] Mura F, Cirigliano A, Maras D and Rinaldi T, 2021 Analysis of moonmilk nanofibers in the etruscan tombs of Tarquinia, *AIP Conference Proceedings* **2416** 020014.
[12] https://www.nenovision.com/
[13] Cecchini A, Adamo F, Buranelli F and Cataldi M 2012 *Le tombe dipinte di Tarquinia: vicenda conservativa, restauri, tecnica di esecuzione.* (Firenze: Nardini Editore).

[14] Mura F, Cirigliano A, Bracciale MP and Rinaldi T 2020 Characterization of nanostructured calcium carbonate found in two ancient Etruscan tombs *AIP Conference Proceedings* **2257** 020011.
[15] Cirigliano A, Tomassetti MC, Di Pietro M, Mura F, Maneschi ML, Gentili MD, Cardazzo B, Arrighi C, Mazzoni C, Negri R and Rinaldi T 2018 Calcite moonmilk of microbial origin in the Etruscan Tomba degli Scudi in Tarquinia, Italy *Scientific reports* **8(1)** pp. 1-10.
[16] Cirigliano A, Mura F, Cecchini A, Tomassetti M, Maras D, Paola FD, Meriggi N, Cavalieri D, Negri R, Quagliariello A, Hallsworth J and Rinaldi T 2020 Active microbial ecosystem in Iron-Age tombs of the Etruscan civilization. *Environmental Microbiology* **23(7)** pp. 3957-3969.
[17] Dufresne WJB, Rufledt CJ and Marshall CP 2018 Raman spectroscopy of the eight natural carbonate minerals of calcite structure *Journal of Raman Spectroscopy* **49** pp. 1999-2007.
[18] Porto SPS., Giordmaine JA and Damen TC 1966 Depolarization of Raman Scattering in Calcite *Physical Review* **147(2)** pp. 608-611.
[19] Liu LG and Mernagh TP 1990 Phase transitions and Raman spectra of calcite at high pressures and room temperature. *American Mineralogist* **75** pp. 801-806.